DYNAMICAL MEAN-FIELD THEORY FOR CORRELATED LATTICE FERMIONS

K. BYCZUK

(1) Theoretical Physics III, Center for Electronic Correlations and Magnetism, Institute for Physics, University of Augsburg, 86135 Augsburg, Germany

(2) Institute of Theoretical Physics, Warsaw University, ul. Hoża 69, 00-681 Warszawa, Poland

Dynamical mean-field theory (DMFT) is a successful method to investigate interacting lattice fermions. In these lecture notes we present an introduction into the DMFT for lattice fermions with interaction, disorder and external inhomogeneous potentials. This formulation is applicable to electrons in solids and to cold fermionic atoms in optical lattices. We review here our investigations of the Mott-Hubbard and Anderson metal-insulator transitions in correlated, disordered systems by presenting selected surprising results.

1. Introduction

The exceptional properties of strongly correlated electron systems have fascinated physicists for several decades already.[1–10] New correlated electron materials and unexpected correlation phenomena are discovered every year. Often the properties of those systems are influenced by disorder. Also inhomogeneous external potentials or layers and interfaces are present in particular experimental realizations, e.g see in [11]. Unfortunately, real materials and even model systems with strong electronic correlations and randomness or inhomogeneities are notoriously hard to investigate theoretically because standard approximations are invalid in the most interesting parameter regime – that of intermediate coupling. Here the recently developed dynamical mean-field theory (DMFT)[12–21] has proved to be an almost ideal mean-field approximation since it may be used at arbitrary coupling. For this reason the DMFT has been successfully employed in the investigation of electronic correlation effects in theoretical models and even real materials.[19–21]

In the present lecture notes we provide an introduction into the DMFT for correlated and disordered electron systems in the inhomogeneous external potential. We start with a brief description of the correlated and disordered electron systems and their models. The DMFT is introduced from the practical point of view. The emphasis is put on the physical interpretation rather then on a formal mathematical structure of the theory. Different approaches to deal with randomness in many-body systems are discussed on the physical ground. The second part of these notes present selected applications of the DMFT for correlated and disordered systems based on our research.

2. Correlation and correlated electron systems

2.1. *Correlations*

The word *correlation* comes from Latin and means "with relation". It implies that at least two objects are in a relation with each other. In mathematics and statistics or natural sciences the correlation has a rigorous meaning.[22] Namely, two random variables x and y are correlated if the average (expectation value) $\langle xy\rangle$ cannot be written as a product of the averages $\langle x\rangle\langle y\rangle$, i.e. explicitly:

$$\langle xy\rangle \neq \langle x\rangle\langle y\rangle\,. \tag{1}$$

In other words, the covariance $cov(x,y) \equiv \langle (x-\langle x\rangle)(y-\langle y\rangle)\rangle \neq 0$. In such a case the probability distribution function $P(x,y)$ cannot be expressed as a product of marginal distribution functions $P_x(x)$ and $P_y(y)$. Of course, the lack of correlations, i.e. $\langle xy\rangle = \langle x\rangle\langle y\rangle$, does not automatically imply that x and y are independent random variables.

To illustrate the concept of correlations imagine a crowd of pedestrians going on a sidewalk in different directions. For each person the walk is deterministic. However, for an observer the walk of a single person X is described by a random variable - the position $\mathbf{r}_X(t)$ at a given time t. Of course, to avoid collisions people make the trajectories mutually dependent. In a statistical analysis of such a system the observer finds that the correlation function of two positions is not factorized $\langle \mathbf{r}_X(t)\mathbf{r}_Y(t')\rangle \neq \langle \mathbf{r}_X(t)\rangle\langle \mathbf{r}_Y(t')\rangle$. It means that the pedestrian motion in a dense crowd is correlated. The same holds true for a motion of cars or airplanes, for example. Dealing with correlations in modelling of such complex systems is a difficult task and requires very sophisticated mathematical techniques.[23]

2.2. *Weakly correlated many-particle systems*

In condensed matter physics we want to model systems containing moles of particles, i.e. of the order 10^{23} in each cube centimeter. A typical course of many-body physics starts from discussing the noninteracting particles.[24] The goal is to find the probability distribution function $f(\mathbf{k})$ describing how particles are distributed over different momenta $\mathbf{k}$. The classical particles are uncorrelated in the absence of interaction and the distribution function is given by the Maxwell-Boltzmann formula. Quantum mechanics introduces new idea: the indistinguishability of identical particles. Then, the distribution function for fermions is given by the Fermi-Dirac formula and for bosons by the Bose-Einstein one. Even then in quantum mechanics, when the interaction is absent, the distribution functions at different momenta are still uncorrelated.

In reality electrons, atoms, and/or protons in condensed matter (liquids, solids, ultracold gases of atoms, nuclei, or nuclear matter in stars) interact with each other by long-range Coulomb and/or short-range strong (nuclear) forces. Often the long-range Coulomb interaction is effectively screened and only the short-range potentials remain. Even then models of such many-body systems are not exactly solvable. An approximation which neglects correlations between the relevant variables is often employed. For example, it is assumed for the density-density correlation function that

$$\langle \rho(\mathbf{r},t)\rho(\mathbf{r}',t')\rangle \approx \langle \rho(\mathbf{r},t)\rangle\langle \rho(\mathbf{r}',t')\rangle\,, \tag{2}$$

where $\rho(\mathbf{r},t)$ is a density of the particles and the expectation values $\langle ...\rangle$ are taken with respect to the quantum mechanical and thermal states. Such factorizing approximation is known as a *Weiss mean-field* type or as a *Hartree-Fock mean-field* type approximation.[25] In these types of theories particles are kept independent from each others and their mutual interaction is included by an average mean-field potential. Saying differently, the independent particle propagates in a mean-field potential created by all other particles.

Nowadays the density functional theory (DFT) is routinely used to explain or predict properties of various interacting many-body systems.[26] In principle, this is an exact, mathematical theory of many particles. However, any practical calculation within DFT uses a mean-field type approximation. The most common one is the local density approximation (LDA) which uses the average charge and spin density distributions to define electric and magnetic mean-field potentials.[27] Although approximate, the DFT with LDA gives a very accurate description, even on a quantitative level, of many bulk

systems as well as molecules and atoms.[26]

2.3. *Strongly correlated many-particle systems*

There are various classes of systems, however, containing either transition metal elements (e.g., Ni, La_2CuO_4, V_2O_3, or NiS_2Se),[8] or Latinate and Actinide elements (e.g., CeCu2Si2, UBe13, or UPt3, commonly named as heavy-fermions),[28,29] which are not described by a theory which neglects electronic correlations. These systems are named *strongly correlated electron systems*. Many examples of correlated electron systems, including high - temperature superconductors with coper-oxygen planes, are reviewed and discussed in Ref. [8].

The canonical example of correlated electron system is V_2O_3.[30] Its phase diagram is presented in Fig. 1. The DFT within LDA predicts that this system is a metal with half-filled conducting band. In experiments however, changing the temperature between 200 and 400K at ambient pressure (see left panel in Fig. 1) one find a huge (8 orders of magnitude) drop of the resistivity at around 150K (see right panel in Fig. 1). The observed phenomenon is an example of the Mott-Hubbard metal insulator transition (MIT) driven by the electronic correlations. The low-temperature paramagnetic Mott insulator is not describe by the DFT with LDA. Also the high-temperature correlated metallic phase is different from that predicted by DFT within LDA, in particular the effective electron mass is strongly enhanced.[10]

The strongly correlated electrons are usually found in systems with partially filled d- or f-orbitals. To understand this we consider a hopping probability amplitude t_{ij} between two sites i and j on a crystal lattice. It is expressed by the overlap matrix element containing the one-particle part of the Hamiltonian $\hat{T}$, i.e. $t_{ij} = \langle i|\hat{T}|j\rangle$, where $|i\rangle$ are Wannier localized wave functions centered at sites i. These hopping amplitudes determine the total band-width W and the average kinetic energy of the electrons. The mean time τ spent by the electron on a given atomic orbital is inversely proportional to the band-width, i.e. $\tau \sim \hbar/W$.[32] For narrow band systems, such as those with partially filled d- or f-orbitals, this mean time τ is large. Hence, the effects due to the interaction with other electrons at the same orbital become very important. The dynamics of a single electron must be correlated with the other electrons. Any theory, which neglects those correlations, fails to explain the existence of Mott insulators and Mott-Hubbard MIT.

Optical lattices (crystal type structures made of standing laser lights)

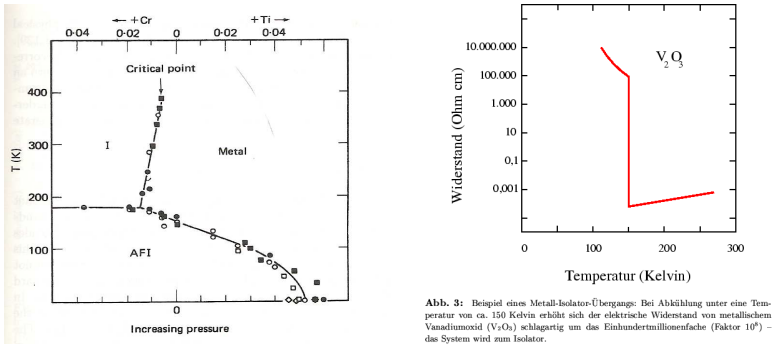

Abb. 3: Beispiel eines Metall-Isolator-Übergangs: Bei Abkühlung unter eine Temperatur von ca. 150 Kelvin erhöht sich der elektrische Widerstand von metallischem Vanadiumoxid (V_2O_3) schlagartig um das Einhundertmillionenfache (Faktor 10^8) – das System wird zum Isolator.

Fig. 1. Left: Phase diagram of V_2O_3 on pressure-temperature (p-T) plane.[30] The low temperature phase is a long-range antiferromagnetic insulator which disappears only at high pressures. At higher temperatures, when the system is paramagnetic one finds a spectacular meta-insulator transition when changing p at constant T or vice versa. Note that substitution of Cr or Ti in position of V acts like internal pressure as long as the system remains isoelectronic. Right: Drop of the resistivity by 8 orders of magnitudes when the metal-insulator transition occurs.[31]

filled with neutral fermionic atoms (e.g., ^{6}Li, ^{40}K, or ^{171}Yb) provide another experimental systems for studying correlated lattice fermions.[33] The relevant system parameters in these artificial crystals can be tuned as desired and various possible phases can be investigated. It is now very rapidly developing field of research, where ideas of condensed matter theory comes into the quantum optics and laser physics.[34–36]

2.4. *Correlated fermions and inhomogeneous potentials*

Inhomogeneous external potentials are present both in cold fermionic atoms loaded into optical lattices and in real materials with correlated electrons. Cold atoms are trapped inside the magneto-optical potentials, usually of ellipsoid-like shapes in space.[37] In case of solids, the experiments are often made with the presence of external gates, which produce space-dependent inhomogeneous electric potentials. One of the example is the quantum point contact, which is a narrow, smooth constriction inside a bulk system.[38] In addition, layers, interfaces, and surfaces play very important role and are extensively studied,[11] as for example in the heterostructres made of $LaTiO_3$ (Mott insulator) and $SrTiO_3$ (band insulator).[39]

3. Disorder and disordered electron systems

In correlated electron materials it is a rule rather than an exception that the electrons, apart from strong interactions, are also subject to disorder. The disorder may result from non-stoichiometric composition, as obtained, for example, by doping of manganites ($La_{1-x}Sr_xMnO_3$) and cuprates ($La_{1-x}Sr_xCuO_4$),[8] or in the disulfides $Co_{1-x}Fe_xS_2$ and $Ni_{1-x}Co_xS_2$.[40] In the first two examples, the Sr ions create different potentials in their vicinity which affect the correlated d electrons/holes. In the second set of examples, two different transition metal ions are located at random positions, creating two different atomic levels for the correlated d electrons. In both cases the random positions of different ions break the translational invariance of the lattice, and the number of d electrons/holes varies. As the composition changes so does the randomness, with $x = 0$ or $x = 1$ corresponding to the pure cases. With changing composition the system can undergo various phase transitions. For example, FeS_2 is a pure band insulator which becomes a disordered metal when alloyed with CoS_2, resulting in $Co_{1-x}Fe_xS_2$. This system has a ferromagnetic ground state for a wide range of x with a maximal Curie temperature T_c of 120 K. On the other hand, when CoS_2 (a metallic ferromagnet) is alloyed with NiS_2 to make $Ni_{1-x}Co_xS_2$, the Curie temperature is suppressed and the end compound NiS_2 is a Mott-Hubbard antiferromagnetic insulator with Néel temperature $T_N = 40$ K.

The transport properties of real materials are also strongly influenced by the electronic interaction and randomness.[41] In particular, Coulomb correlations and disorder are both driving forces behind metal–insulator transitions connected with the localization and delocalization of particles. While the Mott–Hubbard MIT is caused by the electronic repulsion,[4] the Anderson MIT is due to coherent backscattering of non-interacting particles from randomly distributed impurities.[42] Furthermore, disorder and interaction effects are known to compete in subtle ways.[41,43,44]

4. Models for correlated, disordered lattice fermions with inhomogeneous potentials

4.1. *Hubbard model*

As we discussed above, in narrow-band systems the interaction between two electrons occupying the same orbital can play a dominant role. Therefore in theoretical modeling, we take into account this local, on-site interaction. In addition, there is a hopping of the electrons between different lattice sites. The simplest lattice model to describe this situation is provided by

the Hubbard Hamiltonian[45]

$$H = \sum_{ij\sigma} t_{ij} c^{\dagger}_{i\sigma} c_{j\sigma} + \sum_{i\sigma} V_i \; n_{i\sigma} + U \sum_{i} n_{i\uparrow} n_{i\downarrow} \, , \tag{3}$$

where $c^{\dagger}_{i\sigma}$ and $c_{i\sigma}$ are the fermionic creation and annihilation operators of the electron with spin $\sigma = \pm 1/2$ at the lattice site i, $n_{i\sigma} = c^{\dagger}_{i\sigma} c_{i\sigma}$ is the particle number operator with eigenvalues 0 or 1, and t_{ij} is the probability amplitude for an electron hopping between lattice sites i and j. The second term describes the additional external potential V_i, which breaks the ideal lattice symmetry. For homogeneous systems we set $V_i = 0$. Due to the third, two-body term, two electrons with opposite spins at the same site increase the system energy by $U > 0$. In (3) only a local part of the Coulomb interaction is included and other longer-range terms are neglected for simplicity.

The hopping and the interacting terms in the Hamiltonian (3) have different, competing effects in homogeneous systems. The first, kinetic part drives the particles to be delocalized, spreading along the whole crystal as Bloch waves. Then, the one-particle wave functions strongly overlap with each other. The second, interacting term keeps the particles staying apart from each other by reducing the number of double occupied sites. In particular, when the number of electrons N_e is the same as the number of lattice sites N_L the interacting term favors a ground state with all sites being single occupied. Then the overlap of one-particle wave functions is strongly reduced.

The occupation of a single site fluctuates in time when both kinetic and interacting terms are finite. The lattice site i can be either empty $|i, 0\rangle$, or single occupied $|i, \sigma\rangle$, or double occupied with two electrons with opposite spins $|i, 2\rangle$, as shown in Fig. 2. The time evolution depends on the ratio U/t and on the average number of electrons per site $n = \langle \sum_{i\sigma} n_{i\sigma} \rangle / N_L$. As we will explain latter, the DMFT keeps this local dynamics exactly at each site, which is a key point for describing Mott insulators and Mott-Hubbard MIT.

4.2. *Models for external inhomogeneous potential*

The additional inhomogeneous term V_i in the Hamiltonian (3) allows us to model different physical systems. Cold fermionic atoms in optical lattices are trapped by the magneto-optical potential,[37] which is very well described by a three dimensional ellipsoid

$$V_i = k_x (R^x_i - R^x_0)^2 + k_y (R^y_i - R^y_0)^2 + k_z (R^z_i - R^z_0)^2 \, , \tag{4}$$

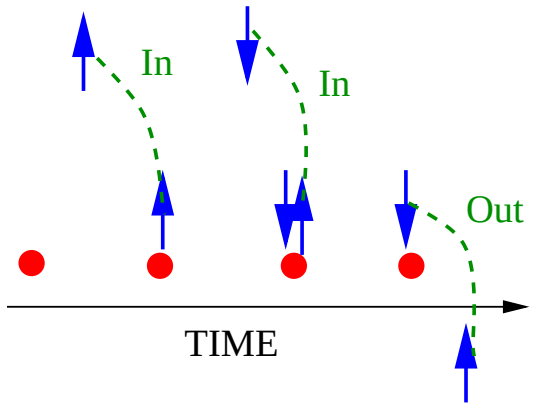

Fig. 2. Evolution of a quantum state at a single lattice site for the electrons described by the Hubbard model (3). The lattice site i can be either empty $|i,0\rangle$, or single occupied $|i,\sigma\rangle$, or double occupied with two electrons with opposite spins $|i,2\rangle$.

centered at the site $\mathbf{R}_0$ and parameterized by three numbers $k_i > 0$. Another choice of the external inhomogeneous potential would describe, for example, a quantum point contact,[38] which is a narrow constriction along the z-direction. Here we model it by a three dimensional hyperboloid potential

$$V_i = -k_x(R_i^x - R_0^x)^2 - k_y(R_i^y - R_0^y)^2 + k_z(R_i^z - R_0^z)^2 \,. \tag{5}$$

Interlayers and thin films or surfaces are modelled by the potential V_i, which changes in a step-wise manner along one selected dimension.[11]

4.3. *Anderson model*

For modelling disordered electrons a similar strategy is usually employed as for the interacting problem. We assume that the particles can hop on a regular lattice but the atomic energy ϵ_i at each lattice site is a random variable. The minimal model describing such a case is given by the Anderson Hamiltonian[42]

$$H = \sum_{ij,\sigma} t_{ij} c_{i\sigma}^\dagger c_{j\sigma} + \sum_{i\sigma} V_i \; n_{i\sigma} + \sum_{i\sigma} \epsilon_i \; n_{i\sigma} \,, \tag{6}$$

where the meanings of the first two terms are the same as in the Eq. (3). In fact, this is a one-body Hamiltonian without any two-body interaction. The effect of disorder on the system is taken into account through a local random term, for which we have to assume a probability distribution function (PDF) .

Typically we consider the uncorrelated quenched disorder with

$$\mathcal{P}(\epsilon_1, ..., \epsilon_{N_L}) = \prod_{i=1}^{N_L} P(\epsilon_i)\,, \tag{7}$$

where $P(\epsilon_i)$ is a normalized PDF for the atomic energies ϵ_i. The quenched disorder means that $P(\epsilon_i)$ is time independent. The atomic energies are randomly distributed over the lattice but then are fixed and cannot be changed. This is different from the annealed disorder where the random atomic energies are supposed to change in time.

4.4. *Models for disorders*

If $P(\epsilon_i) = \delta(\epsilon_i)$, where $\delta(x)$ is a delta-Dirac function, the system is *pure*, i.e. without any disorder. For binary alloy disorder we assume the PDF has the form

$$P(\epsilon_i) = x\delta\left(\epsilon_i + \frac{\Delta}{2}\right) + (1-x)\delta\left(\epsilon_i - \frac{\Delta}{2}\right)\,, \tag{8}$$

where Δ is the energy difference between the two atomic energies , while x and $1-x$ are concentrations of the two alloy atoms. At $x = 0$ or 1 the system is non-disordered even when Δ is finite. Therefore the proper measure of the disorder strength would be a combination $\delta \equiv x(1-x)\Delta$.[46] This model of disorder is applicable to binary alloy A_xB_{1-x} systems, e.g. Ni_xFe_{1-x}. Another choice is a model with the continuous PDF describing continuous disorder. Here we use the box-type PDF

$$P(\epsilon_i) = \frac{1}{\Delta}\Theta(\frac{\Delta}{2} - |\epsilon_i|)\,, \tag{9}$$

with Θ as the step function. The parameter Δ is a measure of the disorder strength. Physics described by these two PDFs is qualitatively different as we shall see further. However, the use of a different continuous, normalized function for the PDF would bring about only quantitative changes.

4.5. *Anderson-Hubbard model*

To describe both correlations and disorder we simply merge together these two Hamiltonians (3) and (6) obtaining so called the Anderson-Hubbard Hamiltonian

$$H = \sum_{ij,\sigma} t_{ij} c^\dagger_{i\sigma} c_{j\sigma} + \sum_{i\sigma} V_i\, n_{i\sigma} \sum_{i\sigma} \epsilon_i\, n_{i\sigma} + U \sum_i n_{i\uparrow} n_{i\downarrow}\,. \tag{10}$$

This model is a working horse for us to investigate the competition between correlations and disorder in lattice fermions.[47–50]

4.6. *Anderson-Falicov-Kimball model*

We also investigate here the spinless Anderson-Falicov-Kimball Hamiltonian

$$H = \sum_{ij} t_{ij} c_i^\dagger c_j + \sum_i V_i \; c_i^\dagger c_i + \sum_i \epsilon_i \; c_i^\dagger c_i + U \sum_i f_i^\dagger f_i c_i^\dagger c_i \,, \qquad (11)$$

where $c_i^\dagger$ ($f_i^\dagger$) and c_i (f_i) are fermionic creation and annihilation operators for *mobile* (*immobile*) fermions at a lattice site i. Furthermore, t_{ij} is the hopping amplitude for mobile particles between sites i and j, and U is the local interaction energy between mobile and immobile particles occupying the same lattice site. The atomic energy ϵ_i is again a random, independent variable which describes the local, *quenched disorder* affecting the motion of mobile particles. Note that imobile fermions are thermodynamically coupled to mobile particles and therefore they act as an annealed disorder.

The Falicov-Kimball Hamilonian without disorder was introduced to model the f- and s-electrons in rare-earth solids, see for review [51], and later generalized for systems with quenched disorder.[52] It can also be realized experimentally using optical lattices filled with light (Li) and heavy (Rb) fermionic atoms, where the relevant parameters are fine tuned by changing the external potentials and magnetic field around the Feschbach resonance.[53] Pure Falicov-Kimball model was studied within the DMFT[51] and also within exact approaches, e.g. [54], or Monte Carlo simulations.[55] This model can also be generalized to include many orbitals[51,56] and exchange interactions.[57]

5. Average over disorder

5.1. *Average and most probable value*

Imagine now a system, described by one of the above Hamiltonians, with a given and fixed distribution of atomic energies over the lattice sites: $\{\epsilon_1, ..., \epsilon_{N_L}\}$. Even if by some means we solve the Hamiltonian, results will depend on this particular realization of the disorder. Different distributions of atoms will give different results. Usually, when the system is infinitely large ($N_L \to \infty$) we take an arithmetic average of the physical quantity (observable) $O(\epsilon_1, ..., \epsilon_{N_L})$ over infinitely may realizations of the disorder, i.e.

$$\langle O(\epsilon) \rangle = \int \prod_{i=1}^{N_L} d\epsilon_i P(\epsilon_i) O(\epsilon_1, ..., \epsilon_{N_L}) \,, \qquad (12)$$

in accord with the Central Limit Theorem[58] for infinitely many, independent random variables $O(\epsilon_1, ..., \epsilon_{N_L})$. Such methodology holds only if the system is self-averaging. It means that the sample-to-sample fluctuations

$$D_{N_L}(O) = \frac{\langle O^2 \rangle - \langle O \rangle^2}{\langle O \rangle^2} \tag{13}$$

vanish when $N_L \to \infty$.

An example of the non-self-averaging system is an Anderson insulator, where the one-particle wave functions are exponentially localized in a finite subsystem.[42] In other words, during the dynamical evolution a quantum state cannot penetrate the full phase space, probing all possible random distributions. Here we are faced with a problem how to describe such systems. In principle, we should investigate the PDF for a given physical observable $O(\epsilon_1, ..., \epsilon_{N_L})$[59] and find the *most probable value* of the observable $O(\epsilon_1, ..., \epsilon_{N_L})$, i.e. such value where the PDF is maximal. This value will represent *typical behavior* of the system. It requires to have a very good statistics, which is based on many (perhaps infinitely many) samples. Such requirement is hardly to achieve, in particular in correlated electron systems, because the relevant Hilbert space is too large to be effectively dealt with. Therefore in practice, we look at a generalized mean which gives the best approximation to this most probable value, e.g. see in [50].

5.2. *Generalized mean*

Generalized f-mean for a single random variable x with a PDF given by $p(x)$ is defined as follows

$$\langle x \rangle_f = f^{-1}(\langle f(x) \rangle)\,, \tag{14}$$

where f and f^{-1} is a function and its inverse.[60,61] The average inside the function f^{-1} is the arithmetic mean with respect to $p(x)$. The geometric mean is obtained when $f(x) = \ln x$.

If $f(x) = x^p$ is a power function of x, the corresponding generalized average is known as a Hölder mean[61] or p-mean

$$\langle x \rangle_p = \left[\int dx p(x) x^p \right]^{\frac{1}{p}}\,, \tag{15}$$

which is parameterized by a single number p. Like the arithmetical mean, the Hölder mean:

- is a homogeneous function of x, and

- have a block property, i.e. $\langle xy\rangle_p = \langle x\rangle_p\langle y\rangle_p$ if x and y are independent random variables.

In particular, it can be seen that $p = -\infty$ gives the possible minimum of x, $p = -1$ gives the harmonic mean, $p = 0$ gives the geometric mean, $p = 1$ is the arithmetic mean, $p = 2$ gives the quadratic mean, and $p = \infty$ gives the maximum of possible x.

Which mean gives the best approximation, in particular when disorder is very strong and drives the system from the self-averaging limit, is a matter of experience and tries. For example, many biological and social processes are modelled by the log-normal PDF, for which the geometrical mean gives exactly the most probable value of the random variable.[62,63] The same is also true for a system of conductors in series with random resistances.

6. Static mean-field theory

6.1. *Exchange Hamiltonian*

Before reviewing the DMFT for correlated fermions we discuss the static (Weiss) mean-field approximation for magnetic systems. This helps to appreciate similarities and differences between the static and the dynamical mean-field theories.

At large U the Hubbard model (3) can be reduced, via the canonical transformation projecting out double occupied sites, to the t-J Hamiltonians with spin-exchange interactions between the electrons.[64] At half-filling the t-J model is exactly equivalent to the Heisenberg Hamiltonian for localized magnetic moments

$$H_{\rm exch} = -\frac{1}{2}\sum_{ij} J_{ij}\mathbf{S}_i\cdot\mathbf{S}_j\,, \tag{16}$$

where $\mathbf{S}_i$ is a quantum mechanical spin operator and $J_{ij} = 4t_{ij}^2/U \ll t_{ij}$ is a kinetic exchange coupling.

6.2. *Static mean-field approximation*

The idea of any mean-field theory is to replace an unsolvable many-body Hamiltonian by a solvable one-body Hamiltonian $H_{\rm MF}$ containing an external fictitious field. In the case of the Heisenberg model (16), we rewrite the partition function as

$$Z = {\rm Tr}_{\mathbf{S}_i} e^{-\beta H_{\rm exch}} = {\rm Tr}_{\mathbf{S}_i} e^{-\beta H_{\rm MF}}\,, \tag{17}$$

where $\beta = 1/kT$ is the inverse of the temperature kT in energy units and Tr denotes the trace over the spin degrees of freedom. The one-body mean-field Hamiltonian $H_{\rm MF}$ is assumed to be

$$H_{\rm MF} = \sum_i \mathbf{B}_i^{\rm MF} \cdot \mathbf{S}_i + E_{shift} \,. \tag{18}$$

The interpretation of (18) is straightforward: localized moments interact only with the external magnetic (Weiss, molecular) mean-field $\mathbf{B}_i^{\rm MF}$. The transformation from the Hamiltonian (16) into the mean-field Hamiltonian (18) is exact from the formal point of view. However, the static Weiss mean-field $\mathbf{B}_i^{\rm MF}$ is not known yet and has to be found within an approximation scheme.

We determine the molecular field within the mean-field (decoupling) approximation $\mathbf{S}_i \cdot \mathbf{S}_j \approx \langle \mathbf{S}_i \rangle \cdot \mathbf{S}_j$. Hence, $\mathbf{B}_i^{\rm MF} = \sum_{j(i)} J_{ij} \langle \mathbf{S}_j \rangle_{H_{\rm MF}}$. Now the average spin $\langle \mathbf{S}_i \rangle$ is found by the self-consistent equation

$$\langle S^z \rangle_{H_{MF}} = \tanh \left(\beta J \langle S^z \rangle_{H_{MF}} \right) \,, \tag{19}$$

where the unknown quantity appears on both sides of it. In the last step we assumed also that the interaction is only between nearest neighbor moments and that the systems is homogeneous. We can solve Eq. (19) iteratively, in the l-th step we plug $\langle S^z \rangle^l_{H_{MF}}$ into the right hand side of (19) and determine new $\langle S^z \rangle^{l+1}_{H_{MF}}$ from the left hand side of (19). We shall repeat this until l-th and l+1-th results are numerically the same with pre-assumed accuracy.

The only approximation within this static mean-field theory is that we have neglected spatial spin-spin correlations, i.e. we have assumed explicitly that

$$\langle [\mathbf{S}_i - \langle \mathbf{S}_i \rangle] \cdot [\mathbf{S}_j - \langle \mathbf{S}_j \rangle] \rangle = 0 \Longrightarrow \langle \mathbf{S}_i \cdot \mathbf{S}_j \rangle = \langle \mathbf{S}_i \rangle \cdot \langle \mathbf{S}_j \rangle \,. \tag{20}$$

It means that a single spin interacts now with an average (mean) external magnetic field, produced by all other spins as is plotted schematically in Fig. 3.

6.3. *Large dimensional limit*

This approximation becomes exact when the single spin interacts with infinitely many other spins. For this either the exchange coupling $J_{ij} = t_{ij}^2/U$ has to be infinitely long-range or there has to be infinitely many nearest neighbors to a given site. The former would lead to hopping amplitudes with pathological properties. The latter is admissible in view of a physical realization. Indeed, note that for the two-dimensional simple cubic (sc) lattice the coordination number $z = 4$, for the three-dimensional simple cubic

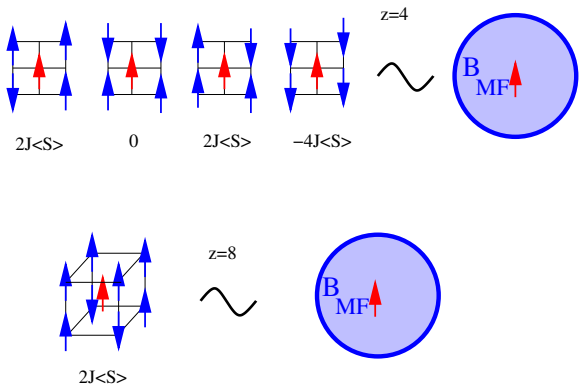

Fig. 3. Different spin configurations are replaced by a single central spin interacting with a mean magnetic field $B^{\rm MF}$. The more spins interact with the central one the more accurate is such approximation.

lattice $z = 6$, for the body centered cubic (bcc) lattice $z = 8$, whereas for the the three-dimensional face centered cubic lattice (fcc) $z = 12$. Large z limit corresponds to the existence of a small, dimensionless parameter $1/z$ in the theory, which vanishes when $z \to \infty$.

The best strategy is to construct a mean-field type theory which is exact in the $z \to \infty$ limit. In practice, a useful non-trivial theory is only obtained when we rescale the exchange coupling, $J = J^*/z$ where $J^* = \text{const}$. In this case the static mean-magnetic field

$$\mathbf{B}^{\rm MF} = \sum_{j=1}^{z} J\langle \mathbf{S}\rangle_{H_{MF}} = \frac{J^*}{z}\sum_{j=1}^{z}\langle \mathbf{S}\rangle_{H_{\rm MF}} = J^*\langle \mathbf{S}\rangle_{H_{\rm MF}} \tag{21}$$

is finite (bounded) in $z \to \infty$ limit. Then the spatial correlations exactly vanish

$$\lim_{z\to\infty}\langle[\mathbf{S}_i - \langle\mathbf{S}_i\rangle]\cdot[\mathbf{S}_j - \langle\mathbf{S}_j\rangle]\rangle = 0 \Longrightarrow \lim_{z\to\infty}\langle\mathbf{S}_i\cdot\mathbf{S}_j\rangle = \langle\mathbf{S}_i\rangle\cdot\langle\mathbf{S}_j\rangle\,. \tag{22}$$

In principle, we can also find corrections to the $z \to \infty$ limit by applying a perturbation theory with respect to $1/z$. Hence, this static mean-field theory is a controlled approximation with well defined small parameter.

Unfortunately this is not the theory which we expect to have for the Hubbard model of correlated fermions. The static mean-field theory was constructed only for the t-J model, where $t \ll U$. On the other hand, as we discussed in the beginning sections, the interesting physics with Mott-Hubbard MIT occurs when $t \sim U$, i.e. in the intermediate coupling regime.

Then the local dynamics seems to be important and we need a dynamical theory, which incorporates those local quantum fluctuations.

7. The Holy Grail for lattice fermions or bosons

In the lack of exact solutions to the interesting models (3,6,10,11) in two or three dimensions, we search for an approximate but comprehensive mean-field theory that:

- is valid for all values of parameters, e.g. U/t, the electron density, disorder strength Δ and concentration x, or temperature;
- is thermodynamically consistent, i.e. irrespectively in which way thermodynamical quantities are calculated, final results are identical;
- is conserving, i.e. the approximation must preserve the microscopic conservation laws of the Hamiltonian;
- has a small controlled (expansion) parameter z and the approximate theory is exact when $z \to \infty$;
- is flexible in application to various classes of correlated fermion models, with and without disorder, and useful to realistic, material specific calculations.

Among many different approximate theories for the Hubbard-like models of lattice fermions, the DMFT is the only one which satisfies all of those requirements.[11,17–21,51] Recently, the bosonic dynamical mean-field theory (B-DMFT) for correlated lattice bosons in normal and Bose-Einstein condensate phases has also been formulated.[65]

8. DMFT - practical and quick formulation

In this Section we discuss the comprehensive mean-field theory for the correlated lattice fermions with disorder and inhomogeneous external potentials. We present a quick and practical formulation of the DMFT equations, which emphasizes the mean-field character of the theory.

8.1. *Exact partition function, Green function, and self-energy*

We begin with the exact partition function for a given lattice problem, e.g. as that described by one of the Hamiltonians (3,6,10,11),

$$Z = \mathrm{Tr} e^{-\beta(H-\mu N)} = \prod_{\sigma\omega_n} \mathrm{Det}[-\hat{G}_\sigma(\omega_n)^{-1}] = \exp\left(\sum_{\sigma\omega_n} \mathrm{Tr}\ln[-\hat{G}_\sigma(\omega_n)^{-1}]\right). \tag{23}$$

This partition function is derived in the Appendix, cf. Eq. (50). Odd Matsubara frequencies $\omega_n = (2n+1)\pi/\beta$, corresponding to the imaginary time τ by the Fourier transform, keep track of the Fermi-Dirac statistics. The hat symbol in $\hat{G}$ reminds us that the Green function is an infinite matrix when expressed in the basis of one-particle wave functions.

Our goal is to formulate the DMFT for arbitrary discrete systems, where the lattice is not necessary of Bravais type.[66–68] Therefore we work with a general quantum numbers α, corresponding to the one-particle basis $|\alpha\rangle$ which diagonalizes the equations of motion, see the Eq. (48) in the Appendix. In particular, the present general formulation of the DMFT is applicable: to regular crystals, where the basis functions are Bloch waves with quasi-momenta $\mathbf{k}$ as proper quantum numbers, as well as to thin films, interlayers, and surfaces,[11,69–71] or to irregular constrictions for electrons and magneto-optical traps for cold atoms, or to infinite graphs, e.g. the Bethe tree with different hoppings.[72,73] We only demand that the lattice is infinitely large since we work directly in the thermodynamic limit.

According to the Dyson equation,[74] the one-particle Green function

$$G_{ij\sigma}(\tau) = -\langle T_\tau c_{i\sigma}(\tau) c^\dagger_{j\sigma}(0)\rangle\,, \tag{24}$$

where T_τ is a chronological operator, can be expressed exactly by the non-interacting Green function $G^0_{ij\sigma}(\omega_n)$ and the self-energy $\Sigma_{ij\sigma}(\omega_n)$, i.e.

$$G_{ij\sigma}(\omega_n)^{-1} = G^0_{ij\sigma}(\omega_n)^{-1} - \Sigma_{ij\sigma}(\omega_n) \tag{25}$$

Here the non-interacting Green function can be written in the $|\alpha\rangle$ basis $G^0_{\alpha\sigma}(\omega_n) = 1/(i\omega_n + \mu - \epsilon_\alpha)$, where ϵ_α are exact eigenvalues of the non-interacting and non-disorder part H_0 of the corresponding Hamiltonian, i.e. $H_0|\alpha\rangle = \epsilon_\alpha|\alpha\rangle$. Then, the partition function (23) is expressed by the exact self-energy

$$Z = \exp\left(\sum_{\sigma\omega_n} \mathrm{Tr}\ln[\hat{G}^0_\sigma(i\omega_n)^{-1} - \hat{\Sigma}_\sigma(\omega_n)]\right). \tag{26}$$

The problem would be solved exactly if we had only known the self-energy $\hat{\Sigma}_\sigma(\omega_n)$.

8.2. *DMFT approximation*

Unfortunately, the self-energy is not known so we have to determine it approximately. Within the DMFT for homogeneous systems we make the main assumption, namely, that the self-energy is α-*independent*, i.e.

$$\Sigma_{\alpha\alpha'\sigma}(\omega_n) = \Sigma_\sigma(\omega_n)\delta_{\alpha\alpha'} \,. \tag{27}$$

For the electrons on Bravais lattices it means that the self-energy is *momentum independent*. Correspondingly in the lattice space, the self-energy is *local*, i.e. only diagonal elements are non-vanishing

$$\Sigma_{ij\sigma}(\omega_n) = \sum_{\alpha\alpha'} \langle i|\alpha\rangle \Sigma_{\alpha\alpha'\sigma} \langle \alpha'|j\rangle = \Sigma_\sigma(\omega_n)\delta_{ij} \,, \tag{28}$$

where δ_{ij} is the lattice Kronecker delta, and we used the completeness of the α-basis, i.e. $1 = \sum_\alpha |\alpha\rangle\langle\alpha|$, together with the orthonormality property of the Wannier states.

For lattice systems with additional, non-uniform external potential V_i we have to make different, independent assumption, namely the *self-energy is local and depends explicitly on site indices*, i.e.

$$\Sigma_{ij\sigma}(\omega_n) = \Sigma_{i\sigma}(\omega_n)\delta_{ij} \,. \tag{29}$$

In general such an assumption does not imply that the self-energy in α-basis is diagonal or independent on α.

Within the DMFT we neglect space correlations by assuming that the self-energy is local, diagonal in the lattice space. The local, dynamical correlations, however, are included exactly by keeping the frequency dependence of $\Sigma_{i\sigma}(\omega_n)$, which translates into explicit time-dependence of the self-energy $\Sigma_{i\sigma}(\tau - \tau')$. Local dynamics is preserved by this approximation and therefore we use the name *dynamical mean-field theory*. The DMFT is the equilibrium theory expecting to describe systems in thermal equilibrium (or close to it, within linear response regime). The extension of the DMFT to non-equilibrium situations is a separate problem, currently being developed.[75]

8.3. *Local Green function*

The local Green function $G_{i\sigma}(i\omega_n) \equiv G_{ii\sigma}(i\omega_n)$ is given by the diagonal elements obtained from the matrix Dyson equation

$$G_{ij\sigma}(i\omega_n) = \left[G^0_{ij\sigma}(i\omega_n)^{-1} - \Sigma_{i\sigma}(i\omega_n)\delta_{ij}\right]^{-1} , \tag{30}$$

provided that we know all local self-energies on all lattice sites. This exact expression is applicable to study finite size systems. When the system is infinitely large we have to make other approximation to make the DMFT equation numerically tractable.

8.4. *Local approximation to Dyson equation*

The local (diagonal in a lattice space) Green function can be expressed solely by the local, non-interacting, pure density of states (LDOS) and the self-energy, namely

$$G_{i\sigma}(\omega_n) = \sum_{\alpha} \frac{|\langle\alpha|i\rangle|^2}{i\omega_n + \mu - \epsilon_\alpha - \Sigma_{i\sigma}(\omega_n)} = \int d\epsilon \frac{N_i^0(\epsilon)}{i\omega_n + \mu - \epsilon - \Sigma_{i\sigma}(\omega_n)}, \tag{31}$$

where $N_i^0(\epsilon) = \sum_\alpha |\langle\alpha|i\rangle|^2 \delta(\epsilon - \epsilon_\alpha)$ is the non-interacting LDOS. This expression is obtained by assuming that on all sites the self-energy $\Sigma_{i\sigma}(i\omega_n)$ is the same when calculating $G_{ii\sigma}(i\omega_n)$. For another site R_j we assume the same but now the self-energy should be $\Sigma_{j\sigma}(i\omega_n)$. We call this as a local Dyson equation approximation (LDEA). For a given problem with the external potential V_i the noninteracting, pure LDOS is determined once at the beginning for all lattice sites and then stored in the computer memory. In practice a system of arbitrary size can be studied within this local approximation. This LDOS is the same and site independent for homogeneous lattices.

This assumption is certainly valid as long as the external potential V_i is a slowly-varying function compared with other characteristic length scales, as a lattice constant a and the Fermi wave-length. This is a quasi-classical (Wigner) description where both the α-quantum number in ϵ_α and the R_i-position in $\Sigma_{i\sigma}(\omega_n)$ are used at the same time.

8.5. *Dynamical mean-field function*

The locality of the self-energy has far reaching consequences as we shall see now. We write the local Green function in a different form, i.e.

$$G_{i\sigma}(\omega_n) = \frac{1}{i\omega_n + \mu - \eta_{i\sigma}(\omega_n) - \Sigma_{i\sigma}(\omega_n)}\,, \tag{32}$$

where we introduced frequency dependent function $\eta_{i\sigma}(\omega_n)$. We can interpret $\eta_{i\sigma}(\omega_n)$ as *dynamical mean-field function*. It describes resonant broadenings of single-site levels due to coupling of a given site to the rest of the system. In different words, a coupling of the selected single site to all other

sites is described in average by the local dynamical mean-field function $\eta_{i\sigma}(\omega_n)$.

8.6. *Self-consistency conditions*

The partition function is expressed now as a product of the partition functions determined on each lattice sites

$$Z = \prod_{i=1}^{N_L} Z_i = \prod_{i=1}^{N_L} \exp\left(\sum_{\sigma\omega_n} \ln[i\omega_n + \mu - \eta_{i\sigma}(\omega_n) - \Sigma_{i\sigma}(\omega_n)]\right) . \tag{33}$$

The mean-field function $\eta_{i\sigma}(\omega_n)$ looks formally like an site- and time- dependent potential. In the interaction representation, the unitary time evolution due to this potential is described by the local, time-dependent evolution operator[11,51]

$$U[\eta_{i\sigma}] = T_\tau e^{-\int_0^\beta d\tau \int_0^\beta d\tau' c^\dagger_{i\sigma}(\tau)\eta_{i\sigma}(\tau-\tau')c_{i\sigma}(\tau')} . \tag{34}$$

In the final step we write the partition function (33) as a trace of operators

$$Z = Z[\eta_{i\sigma}] = \prod_{i=1}^{N_L} \mathrm{Tr}\left[e^{-\beta(H_i^{\mathrm{loc}} - \mu N_i^{\mathrm{loc}})} U[\eta_{i\sigma}]\right] , \tag{35}$$

where H_i^{loc} is the local part of the lattice Hamiltonian operator and describes the interaction and/or disorder. Here N_i^{loc} is the local particle number operator. The Eq. (35) is our main result allowing us to determine the interesting, local Green function for a given dynamical mean-field $\eta_{i\sigma}(\omega_n)$. Indeed, the local Green function is obtained by taking a functional derivative of the logarithm from the partition function (35) with respect to $\eta_{i\sigma}(\omega_n)$,[11,51] i.e.

$$G_{i\sigma}(\omega_n) = -\frac{\partial \ln Z[\eta_{i\sigma}]}{\partial \eta_{i\sigma}(\omega_n)} . \tag{36}$$

In systems with disorder, the local part of the Hamiltonian H_i^{loc} has the random variable ϵ_i and therefore the local Green function (36) is also a random quantity. In such a case we determine the average local Green function by taking one of the mean, introduced above. For this we calculate the spectral function, the interacting LDOS, from (36), i.e.

$$A_{i\sigma}(\omega) = -\frac{1}{\pi}\mathrm{Im}G_{i\sigma}(\omega_n \to \omega + i0^+) , \tag{37}$$

and determine we the p-mean with respect to a given PDF

$$\langle A_{i\sigma}(\omega)\rangle_p = \left[\int d\epsilon P(\epsilon) A_{i\sigma}(\omega)^p\right]^{\frac{1}{p}} . \tag{38}$$

According to the spectral representation theorem[74] the averaged local Green function is

$$\langle G_{i\sigma}(\omega_n)\rangle_p = \int d\omega \frac{\langle A_{i\sigma}(\omega)\rangle_p}{i\omega_n - \omega}\,, \tag{39}$$

and should be used instead of (36) is systems with disorder.

Knowing $G_{i\sigma}(\omega_n)$ from the Eq. (36) or its average form from the Eq. (39) we find directly the self-energy from the Eq. (32), i.e.

$$\Sigma_{i\sigma}(\omega_n) = i\omega_n + \mu - \eta_{i\sigma}(\omega_n) - \frac{1}{G_{i\sigma}(\omega_n)}\,, \tag{40}$$

or

$$\Sigma_{i\sigma}(\omega_n) = i\omega_n + \mu - \eta_{i\sigma}(\omega_n) - \frac{1}{\langle G_{i\sigma}(\omega_n)\rangle_p}\,, \tag{41}$$

respectively.

The local Green function is determined for a given, fixed mean-field potential $\eta_{i\sigma}(\omega_n)$. To obtain a self-consistent solution we proceed iteratively by employing the Eq. (31) to obtain a new local Green function, which afterwards is used to determine a new mean-field function from Eq. (32). This should be done on all lattice sites in parallel if the system contains the external, inhomogeneous potential V_i. For Bravais lattices the self-energy is the same on each site so does the mean-field function $\eta_\sigma(\omega_n)$. Then the site index i is irrelevant and can be omitted. The iteration steps should be repeated until the l-th and l+1-th results are numerically the same with a pre-assumed accuracy.

9. Limit of large coordination number

The success of the DMFT can be ascribed to the fact that this theory provides an exact solution for non-trivial lattice Hamiltonians in the limit of large coordination number, i.e. $z \to \infty$. Similarly to the static mean-field theory for the exchange Hamiltonian, in the $z \to \infty$ limit the space correlation functions vanish. The remaining correlations are local but time dependent and completely taken into account by the DMFT.

To obtain a non-trivial theory in the $z \to \infty$ limit the hopping amplitudes in the lattice Hamiltonians have to be rescaled,[12] i.e. $t_{ij} = t^*_{ij}/\sqrt{d^{R_{ij}}}$, where R_{ij} is a distance between sites i and j obtained by counting the minimal number of links between them. Then the non-local hopping, the local interacting, and the local random parts of the Hamiltonians (3,6,10,11) are treated on equal footing.[12–14,19,76] It can be exactly shown that the self-energy is then local. Hence our quick, practical derivation becomes also an

exact solution of the corresponding lattice problem. In addition, it can be shown that within this rescaling scheme, the lattice disordered systems are self-averaging and the use of arithmetic averaging is justified.[76] For uncorrelated disordered systems the DMFT is equivalent to the coherent potential approximation (CPA).[77]

Since the theory is exact in the large z limit it must be conserving and thermodynamically consistent. Also it must give a comprehensive description of full phase diagrams in all possible regimes of the model and external parameters.

We also mention here that DMFT is formulated in such a way as to describe phases with long-range orders.[19] Also the DMFT can be merged with realistic *ab initio* calculations, which is known as the LDA+DMFT approach.[20,21] These examples show flexibility of the DMFT and ability to describe real physical systems.

The DMFT set of equations have to be solved. The most difficult part is determination of the local Green function from the Eq. (35). Apart of the Falicov-Kimball model and similar ones, where there exist additional local conservation laws, the calculation of the partition function (35) and the following Green functions requires advanced numerical approaches. Different techniques are routinely used now and discussed in details in literature.[19] The results presented here were obtained by using Quantum Monte Carlo (QMC) simulations at finite temperatures[19] and Numerical Renormalization Group (NRG) at zero temperature.[78,79]

10. Surprising results from DMFT

The investigations of electronic correlations and their interplay with disorder by means of the DMFT has led us to the discovery of several unexpected properties and phenomena. Examples are: (i) a novel type of Mott-Hubbard metal insulator transition away from integer filling in the presence of binary alloy disorder;[48] (ii) an enhancement of the Curie temperature in correlated electron systems with binary alloy disorder;[47,49] and (iii) unusual effects of correlations and disorder on the Mott-Hubbard and Anderson MITs, respectively.[50,52] Below we describe and explain these often surprising results as an illustration of the theory introduced above.

10.1. *Metal-insulator transition at fractional filling*

The Mott-Hubbard MIT occurs upon increasing the interaction strength U in the models (10) and (11) if the number of electrons N_e is commensurate

with the number of lattice sites N_L or, more precisely, if the ratio N_e/N_L is an odd integer. At zero temperature it is a continuous transition whereas at finite temperatures the transition is of first-order.[19,80] Surprisingly, in the presence of binary alloy disorder the MIT occurs at fractional filling.[48]

We describe this situation by using the Anderson-Hubbard model (10) with the distribution (8) which corresponds to a binary-alloy system composed of two different atoms A and B. The atoms are distributed randomly on the lattice and have ionic energies $\epsilon_{A,B}$, with $\epsilon_B - \epsilon_A = \Delta$. The concentration of A (B) atoms is given by $x = N_A/N_L$ $(1 - x = N_B/N_L)$, where N_A (N_B) is the number of the corresponding atoms.

From the localization theorem (the Hadamard–Gerschgorin theorem in matrix algebra) it is known that if the Hamiltonian (10), with a binary alloy distribution for ϵ_i, is bounded, then there is a gap in the single–particle spectrum for sufficiently large $\Delta \gg \max(|t|,\ U)$. Hence at $\Delta = \Delta_c$ the DOS splits into two parts corresponding to the lower and the upper alloy subbands with centers of mass at the ionic energies ϵ_A and ϵ_B, respectively. The width of the alloy gap is of the order of Δ. The lower and upper alloy subband contains $2xN_L$ and $2(1-x)N_L$ states, respectively.

New possibilities appear in systems with correlated electrons and binary alloy disorder.[48] The Mott–Hubbard metal insulator transition can occur at any filling $n = x$ or $1 + x$, corresponding to a half–filled lower or to a half–filled upper alloy subband, respectively, as shown schematically for $n = x$ in Fig. 4. The Mott insulator can then be approached either by increasing U when $\Delta \geq \Delta_c$ (alloy band splitting limit), or by increasing Δ when $U \geq U_c$ (Hubbard band splitting limit). The nature of the Mott insulator in the binary alloy system can be understood physically as follows. Due to the high energy cost of the order of U the randomly distributed ions with lower (higher) local energies ϵ_i are singly occupied at $n = x$ $(n = 1 + x)$, i.e., the double occupancy is suppressed. In the Mott insulator with $n = x$ the ions with higher local energies are empty and do not contribute to the low–energy processes in the system. Likewise, in the Mott insulator with $n = 1 + x$ the ions with lower local energies are double occupied implying that the lower alloy subband is blocked and does not play any role.

For $U > U_c(\Delta)$ in the Mott insulating state with binary alloy disorder one may use the lowest excitation energies to distinguish two different types of insulators. Namely, for $U < \Delta$ an excitation must overcome the energy gap between the lower and the upper Hubbard subbands, as indicated in Fig. 4. We call this insulating state an *alloy Mott insulator*. On the other hand, for $\Delta < U$ an excitation must overcome the energy gap between the

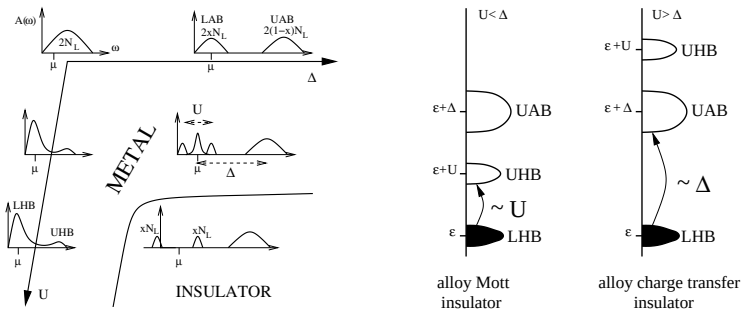

Fig. 4. Left: Schematic plot representing the Mott–Hubbard metal–insulator transition in a correlated electron system with the binary alloy disorder. The shapes of spectral functions $A(\omega)$ are shown for different interactions U and disorder strengths Δ. Increasing Δ at $U = 0$ leads to splitting of the spectral function into the lower (LAB) and the upper (UAB) alloy subbands, which contain $2xN_L$ and $2(1-x)N_L$ states respectively. Increasing U at $\Delta = 0$ leads to the occurrence of lower (LHB) and upper (UHB) Hubbard subbands. The Fermi energy for filling $n = x$ is indicated by μ. At $n = x$ (or $n = 1 + x$, not shown in the plot) the LAB (UAB) is half–filled. In this case an increase of U and Δ leads to the opening of a correlation gap at the Fermi level and the system becomes a Mott insulator. Right: Two possible insulating states in the correlated electron system with binary–alloy disorder. When $U < \Delta$ the insulating state is an alloy Mott insulator with an excitation gap in the spectrum of the order of U. When $U > \Delta$ the insulating state is an alloy charge transfer insulator with an excitation gap of the order of Δ; after Ref. [48]

lower Hubbard subband and the upper alloy–subband, as shown in Fig. 4. We call this insulating state an *alloy charge transfer insulator*.

In Fig. 5 we present a particular phase diagram for the Anderson-Hubbard model at filling $n = 0.5$ showing a Mott-Hubbard type of MIT with typical hysteresis.

10.2. *Disorder-induced enhancement of the Curie temperature*

Itinerant ferromagnetism in the pure Hubbard model occurs only away from half-filling and if the DOS is asymmetric and peaked at the lower edge.[81,82] While the Curie temperature increases with the strength of the electron interaction one would expect it to be lowered by disorder. However, our investigations show that in some cases the Curie temperature can actually be increased by binary alloy disorder.[47,49]

Indeed, the Curie temperature as a function of alloy concentration exhibits very rich and interesting behavior as is shown in Fig. 6. At some concentrations and certain values of U, Δ and n, the Curie temperature is

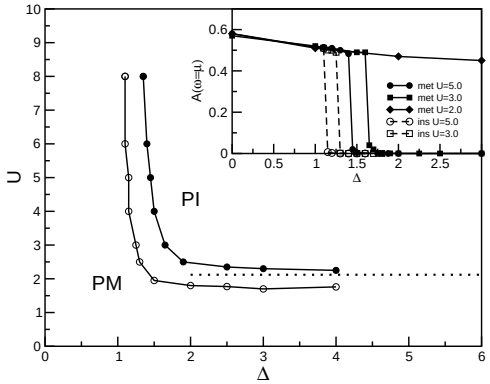

Fig. 5. Ground state phase diagram of the Hubbard model with binary–alloy disorder at filling $n = x = 0.5$. The filled (open) dots represent the boundary between paramagnetic metallic (PM) and paramagnetic insulating (PI) phases as determined by DMFT with the initial input given by the metallic (insulating) hybridization function. The horizontal dotted line represents U_c obtained analytically from an asymptotic theory in the limit $\Delta \to \infty$. Inset: hysteresis in the spectral functions at the Fermi level obtained from DMFT with an initial metallic (insulating) host represented by filled (open) symbols and solid (dashed) lines; after.[48]

enhanced above the corresponding value for the non-disordered case ($x = 0$ or 1). This is shown in the upper panel of Fig. 6 for $0 < x < 0.2$. The relative increase of T_c can be as large as 25%, as is found for $x \approx 0.1$ at $n = 0.7$, $U = 2$ and $\Delta = 4$ (upper panel of Fig. 6).

This unusual enhancement of T_c is caused by three distinct features of interacting electrons in the presence of binary alloy disorder:

i) The Curie temperature in the non-disordered case $T_c^{\rm p} \equiv T_c(\Delta = 0)$, depends non-monotonically on band filling n.[81] Namely, $T_c^{\rm p}(n)$ has a maximum at some filling $n = n^*(U)$, which increases as U is increased; see also our schematic plots in Fig. 7.

ii) As was described above, in the alloy-disordered system the band is split when $\Delta \gg W$. As a consequence, for $n < 2x$ and $T \ll \Delta$ electrons occupy only the lower alloy subband and for $n > 2x$ both the lower and upper alloy subbands are filled. In the former case the upper subband is empty while in the later case the lower subband is completely full. Effectively, one can therefore describe this system by a Hubbard model mapped onto the either lower or the upper alloy subband, respectively. The second subband plays a passive role. Hence, the situation corresponds to a *single* band with the *effective* filling $n_{\rm eff} = n/x$ for $n < 2x$ and $n_{\rm eff} = (n - 2x)/(1 - x)$ for $n > 2x$. It is then possible to determine T_c from the phase diagram of the Hubbard model without disorder.

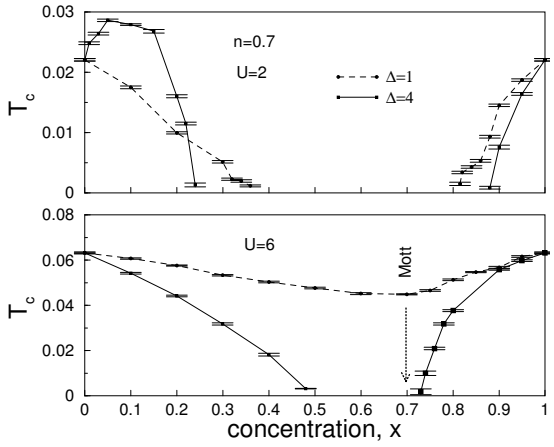

Fig. 6. Curie temperature as a function of alloy concentration x at $U = 2$ (upper panel) and 6 (lower panel) for $n = 0.7$ and disorder $\Delta = 1$ (dashed lines) and 4 (solid lines); after Refs. [47,49].

iii) The disorder leads to a reduction of $T_c^{\rm p}(n_{\rm eff})$ by a factor $\alpha = x$ if the Fermi level is in the lower alloy subband or $\alpha = 1 - x$ if it is in the upper alloy subband, i. e. we find

$$T_c(n) \approx \alpha T_c^{\rm p}(n_{\rm eff})\,, \tag{42}$$

when $\Delta \gg W$. Hence, as illustrated in Fig. 7, T_c can be determined by $T_c^{\rm p}(n_{\rm eff})$. Surprisingly, then, it follows that for suitable U and n the Curie temperature of a disordered system can be higher than that of the corresponding non-disordered system [cf. Fig. 7].

10.3. *Continuously connected insulating phases in strongly correlated systems with disorder*

The Mott-Hubbard MIT is caused by Coulomb correlations in the pure system. By contrast, the Anderson MIT, also referred to as Anderson localization, is due to coherent backscattering from randomly distributed impurities in a system without interaction.[42] It is therefore a challenge to investigate the effect of the *simultaneously* presence of interactions and disorder on electronic systems.[50,52] In particular, the question arises whether it will suppress or enlarge a metallic phase. And what about the Mott and Anderson insulating phases: will they be separated by a metallic phase? Possible scenarios are schematically plotted in Fig. 8.

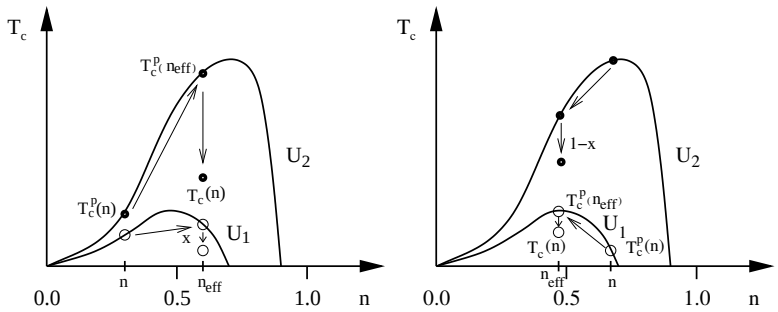

Fig. 7. Schematic plots explaining the filling dependence of T_c for interacting electrons with strong binary alloy disorder. Curves represent $T_c^{\rm p}$, the Curie temperature for the pure system, as a function of filling n at two different interactions $U_1 \ll U_2$. Left: For $n < x$, T_c of the disordered system can be obtained by transforming the open (for U_1) and the filled (for U_2) point from n to $n_{\rm eff} = n/x$, and then multiplying $T_c^{\rm p}(n/x)$ by x as indicated by arrows. One finds $T_c(n) < T_c^{\rm p}(n)$ for U_1, but $T_c(n) > T_c^{\rm p}(n)$ for U_2. Right: For $n > x$, T_c of the disordered system can be obtained by transforming $T_c^p(n)$ from n to $n_{\rm eff} = (n-2x)/(1-x)$, and then multiplying $T_c^{\rm p}[(n-2x)/(1-x)x]$ by $1-x$ as indicated by arrows. One finds $T_c(n) > T_c^{\rm p}(n)$ for U_1, but $T_c(n) < T_c^{\rm p}(n)$ for U_2; after Ref. [47,49].

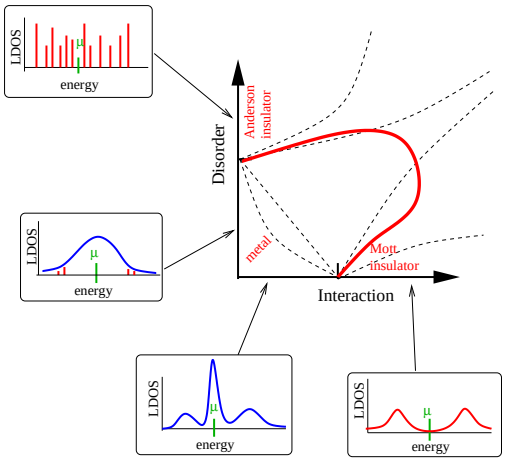

Fig. 8. Possible phases and phase transitions triggered by interaction and disorder in the same system. According to DMFT investigations the simultaneous presence of correlations and disorder enhances the metallic regime (thick line); the two insulating phases are connected continuously. Insets show different local density of states when disorder or interaction is switched off.

The Mott-Hubbard MIT is characterized by the opening of a gap in the density of states at the Fermi level. At the Anderson localization transition

the character of the spectrum at the Fermi level changes from a continuous spectrum to a dense, pure point spectrum. It is plausible to assume that both MITs can be characterized by a single quantity, namely, the local density of states (LDOS). Although the LDOS is not an order parameter associated with a symmetry breaking phase transition, it discriminates between a metal and an insulator, which is driven by correlations and disorder, cf. insets to Fig. 8.

In a disordered system the LDOS depends on a particular realization of the disorder in the system. To obtain a full understanding of the effects of disorder it would therefore in principle be necessary to determine the entire probability distribution function of the LDOS, which is almost never possible. Instead one might try to calculate moments of the LDOS. This, however, is insufficient because the arithmetically averaged LDOS (first moment) stays finite at the Anderson MIT.[83] It was already pointed out by Anderson[42] that the "typical" values of random quantities, which are mathematically given by the most probable values of the probability distribution functions, should be used to describe localization. The *geometric* mean is defined by

$$A_{\rm geom} = \exp\left[\langle \ln A(\epsilon_i)\rangle_{\rm dis}\right] , \tag{43}$$

and differs from the arithmetical mean given by

$$A_{\rm arith} = \langle A(\epsilon_i)\rangle_{\rm dis} , \tag{44}$$

where $\langle F(\epsilon_i)\rangle_{\rm dis} = \int d\epsilon_i \mathcal{P}(\epsilon_i) F(\epsilon_i)$ is an arithmetic mean of function $F(\epsilon_i)$. The geometrical mean gives an approximation of the most probable ("typical") value of the LDOS and vanishes at a critical strength of the disorder, hence providing an explicit criterion for Anderson localization.[42,84–86]

A non-perturbative framework for investigations of the Mott-Hubbard MIT in lattice electrons with a local interaction and disorder is provided by the dynamical mean-field theory (DMFT).[17,19] If in this approach the effect of local disorder is taken into account through the arithmetic mean of the LDOS[87] one obtains, in the absence of interactions, the well known coherent potential approximation (CPA),[76] which does not describe the physics of Anderson localization. To overcome this deficiency Dobrosavljević *et al.*[85] incorporated the geometrically averaged LDOS into the self-consistency cycle and thereby derived a mean-field theory of Anderson localization which reproduces many of the expected features of the disorder-driven MIT for non-interacting electrons. This scheme uses only one-particle quantities and is therefore easily incorporated into the DMFT for disordered electrons in the presence of phonons,[88] or Coulomb correlations.[50,52] In particular,

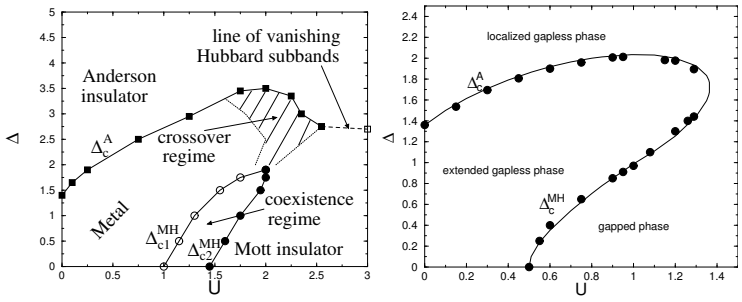

Fig. 9. Non-magnetic ground state phase diagram of the Anderson-Hubbard (left) and Anderson-Falicov-Kimball (right) models at half-filling as calculated by DMFT with the typical local density of states; after Refs. [50,52]

the DMFT with geometrical averaging allows to compute phase diagrams for the Anderson-Hubbard model (10) and the Anderson-Falicov-Kimball model (11) with the continuous probability distribution function (9) at half-filling.[50,52] In this way we found that, although in both models the metallic phase is enhanced for small and intermediate values of the interaction and disorder, metallicity is finally destroyed. Surprisingly, the Mott and Anderson insulators are found to be continuously connected. Phase diagrams for the non-magnetic ground state are shown in Fig. 9. The method based on geometric averaging described here was further investigated in details in Refs. [89–92].

11. Conclusions

The physics of correlated electron systems is known to be extremely rich. Therefore their investigation continues to unravel novel and often surprising phenomena, e.g. formation of kinks in the electronic dispersion relations.[93] The presence of disorder further enhances this complexity. Here we discussed several remarkable features induced by correlations with and without disorder, which came as a surprise when they were first discovered, but which after all have physically intuitive explanations. Behind these discoveries is the dynamical mean-field theory, which was described here for lattice quantum systems with interaction, disorder and external potentials.

Acknowledgments

It is a pleasure to thank R. Bulla, M. Eckstein, W. Hofstetter, A. Kauch, M. Kollar, and in particular D. Vollhardt for many discussions and collab-

orations involving different DMFT projects. This work was supported by the Sonderforschungsbereich 484 of the Deutsche Forschungsgemeinschaft.

12. Appendix

A very convenient method to calculate the fermionic partition function is the path-integral technique[74] invented originally by Feynman. The partition function is represented as a functional integral over anticommuting, time dependent functions

$$Z = Tre^{-\beta(H-\mu N)} = \int D[c^*_{i\sigma}, c_{i\sigma}] e^{-S[c^*_{i\sigma}, c_{i\sigma}]}\,, \tag{45}$$

where the action S is defined explicitly for a given Hamiltonian

$$S[c^*_{i\sigma}, c_{i\sigma}] = \int_0^\beta d\tau \sum_{i\sigma} c^*_{i\sigma}(\tau)(\partial_\tau - \mu) c_{i\sigma}(\tau) + \int_0^\beta d\tau H[c^*_{i\sigma}(\tau), c_{i\sigma}(\tau)]\,, \tag{46}$$

with the antisymmetric boundary condition $c_{i\sigma}(\tau+\beta) = -c_{i\sigma}(\tau)$ to keep the Fermi-Dirac statistics.

In the DMFT we are mainly interested in the one-particle Green function (propagator), which is simply expressed by the functional integral

$$\begin{aligned} G_{ij\sigma}(\tau - \tau') &= -\langle T_\tau c_{i\sigma}(\tau) c^\dagger_{i\sigma}(\tau')\rangle \\ &= -\frac{1}{Z}\int D[c^*_{i\sigma}, c_{i\sigma}] c_{i\sigma}(\tau) c^*_{i\sigma}(\tau') e^{-S[c^*_{i\sigma}, c_{i\sigma}]}\,. \end{aligned} \tag{47}$$

The Green function obeys the equation of motion

$$\left[(\partial_\tau - \mu)\hat{1} + \hat{H}\right]\hat{G}(\tau - \tau') = -\delta(\tau - \tau')\hat{1}\,, \tag{48}$$

where we used the matrix notation for $\hat{G}$ and the Hamiltonian operator $\hat{H}$, whereas $\hat{1}$ is a unit matrix.

With the help of Eq. (48), the exact partition function (45) can be expressed exactly by the Green function

$$Z = \int D[\bar{c}^*, \bar{c}] e^{\int_0^\beta d\tau \int_0^\beta d\tau' \bar{c}^*(\tau)\hat{G}^{-1}(\tau-\tau')\bar{c}(\tau')}\,, \tag{49}$$

where we used compact vector and matrix notations. The Gaussian functional integral is evaluated and we obtain

$$Z = \mathrm{Det}[-\hat{G}^{-1}] = e^{\mathrm{Tr}\ln[-\hat{G}^{-1}]}\,, \tag{50}$$

where the determinant and the trace are taken over relevant quantum numbers and over the imaginary time τ or Matsubara frequencies ω_n, depending which representation we use. This is equivalent because of the Fourier

transform relation

$$\hat{G}(\tau) = \frac{1}{\beta} \sum_{\omega_n} e^{i\omega_n \tau} \hat{G}(\omega_n) \,, \tag{51}$$

where $\omega_n = (2n+1)\pi/\beta$ are odd Matsubara frequencies. The formal expression (50) is our starting point in derivation the DMFT equations.

References

1. J.H. de Boer and E.J.W. Verwey, Proc. Phys. Soc. **49**, No. 4S, 59 (1937).
2. N.F. Mott, Proc. Phys. Soc. **49**, No. 4S, 57 (1937).
3. D. Pines, *The Many-Body Problem*, (W. A. Benjamin, Reading, 1962).
4. N.F. Mott, Proc. Phys. Soc. **A62**, 416 (1949); *Metal–Insulator Transitions*, 2nd edn. (Taylor and Francis, London 1990).
5. D. Vollhardt, *Proceedings of the International School of Physics Enrico Fermi, Course CXXI*, Eds. R. A. Broglia and J. R. Schrieffer, p. 31, (North-Holland, Amsterdam, 1994).
6. P. Fulde, *Electron Correlations in Molecules and Solids*, (Springer, Heidelberg, 1995).
7. F. Gebhard, *The Mott Metal-Insulator Transition*, (Springer, Heidelberg, 1997).
8. M. Imada, A. Fujimori and Y. Tokura, Rev. Mod. Phys. **70**, 1039 (1998).
9. P. Fazekas, *Lecture Notes on Electron Correlation and Magnetism*, (World Scientific, Singapore, 1999).
10. J. Spalek, Eur. J. Phys. **21**, 511 (2000).
11. J.K. Freericks, *Transport in multilayered nanostructures The dynamical mean-field theory approach*, (Imperial College Press, 2006).
12. W. Metzner and D. Vollhardt, Phys. Rev. Lett. **62**, 324 (1989).
13. E. Müller-Hartmann, Z. Phys. **B76**, 211 (1989).
14. V. Janiš, Z. Phys. **B83**, 227 (1991);
    V. Janiš and D. Vollhardt, Int. J. Mod. Phys. **6**, 731 (1992).
15. A. Georges and G. Kotliar, Phys. Rev. **B45**, 6479 (1992).
16. M. Jarrell, Phys. Rev. Lett. **69**, 168 (1992).
17. D. Vollhardt, in *Correlated Electron Systems*, Ed. V.J. Emery, World Scientific, Singapore, 1993, p. 57.
18. Th. Pruschke, M. Jarrell and J. K. Freericks, Adv. in Phys. **44**, 187 (1995).
19. A. Georges, G. Kotliar, W. Krauth and M. J. Rozenberg, Rev. Mod. Phys. **68**, 13 (1996).
20. G. Kotliar and D. Vollhardt, Physics Today **57**, No. 3 (March), 53 (2004).
21. G. Kotliar, S.Y. Savrasov, K. Haule, V.S. Oudovenko, O. Parcollet and C.A. Marianetti, Rev. Mod. Phys. **78**, 865 (2006)
22. Wikipedia, the free encyclopedia:
    http://en.wikipedia.org/wiki/Correlation .
23. E.g.: A. Seyfried, B. Steffen and Th. Lippert, Physica **A368**, 232 (2006).
24. K. Huang, *Statistical mechanics*, (John Wiley and Sons, Inc., 1963, 1987).

25. Wikipedia, the free encyclopedia:
http://en.wikipedia.org/wiki/Mean_field_theory .
26. W. Kohn, Rev. Mod. Phys. **71**, 1253 (1999); Rev. Mod. Phys. **71**, S59 (1999); and references therein.
27. W. Kohn and L.J. Sham, Phys. Rev. **140**, A1133 (1965).
28. G.R. Stewart, Rev. Mod. Phys. **56**, 755 (1984).
29. A.C. Hewson, *The Kondo Problem to Heavy Fermions*, (Cambridge University Press, 1997).
30. D.B. McWhan, A. Menth, J.P. Remeika, W.F. Brinkman and T.M. Rice, Phys. Rev. **B7**, 1920 (1973).
31. D. Vollhardt, UniPress, Zeitschrift der Universität Augsburg, Band 3 und 4, p. 29 (1996); see also:
http://www.physik.uni-augsburg.de/theo3/Research/research_fest.vollha.de.shtml .
32. Indeed, the group velocity v is estimated as $v = a/\tau$, where a is a lattice constant, and using the Heisenberg principle $W\tau \sim \hbar$ we find that $a/\tau \sim aW/\hbar$.
33. I. Bloch, Nature Phys. **1**, 23 (2005);
M. Köhl and T. Esslinger, Europhys. News **37**, 18 (2005).
34. W. Hofstetter, Advances in Solid State Physics **45**, 109 (2005).
35. M. Lewenstein, A. Sanpera, V. Ahufinger, B. Damski, A. Sen De and U. Sen, Advances in Physics **56**, 243 (2007).
36. I. Bloch, J. Dalibard and W. Zwerger, arXiv:0704.3011.
37. W.D. Phillips, Rev. Mod. Phys. **70**, 721 (1998).
38. H. van Houten and C.W.J. Beenakker, Physics Today **49** July, 22 (1996);
C.W.J.Beenakker and H. van Houten, Solid State Physics **44** (1991).
39. A. Ohtomo, D.A. Muller, J.L. Grazul and H.Y. Hwang, Nature **419**, 378 (2002);
M. Takizawa, H. Wadati, K. Tanaka, M. Hashimoto, T. Yoshida, A. Fujimori, A. Chikamtsu, H. Kumigashira, M. Oshima, K. Shibuya, T. Mihara, T. Ohnishi, M. Lippmaa, M. Kawasaki, H. Koinuma, S. Okamoto and A.J. Millis, Phys. Rev. Lett. **97**, 057601 (2006).
40. H.S. Jarrett *et al.*, Phys. Rev. Lett. **21**, 617 (1968);
G.L. Zhao, J. Callaway and M. Hayashibara, Phys. Rev. **B48**, 15781 (1993);
S.K. Kwon, S.J. Youn and B.I. Min, Phys. Rev. **B62**, 357 (2000);
T. Shishidou *et al.*, Phys. Rev. **B64**, 180401 (2001).
41. P.A. Lee and T.V. Ramakrishnan, Rev. Mod. Phys. **57**, 287 (1985);
D. Belitz and T.R. Kirkpatrick, Rev. Mod. Phys. **66**, 261 (1994).
42. P.W. Anderson, Phys. Rev. **109**, 1492 (1958).
43. S.V. Kravchenko *et al.*, Phys. Rev. **B50**, 8039 (1994);
D. Popović, A.B. Fowler and S. Washburn, Phys. Rev. Lett. **79**, 1543 (1997);
S.V. Kravchenko and M.P. Sarachik, Rep. Prog. Phys. **67**, 1 (2004);
H. von Löhneysen, Adv. in Solid State Phys. **40**, 143 (2000).
44. A.M. Finkelshtein, Sov. Phys. JEPT **75**, 97 (1983);
C. Castellani *et al.*, Phys. Rev. **B30**, 527 (1984);
M.A. Tusch and D.E. Logan, Phys. Rev. **B48**, 14843 (1993); ibid. **51**, 11940

(1995);
D.L. Shepelyansky, Phys. Rev. Lett. **73**, 2607 (1994);
P.J.H. Denteneer, R.T. Scalettar and N. Trivedi, Phys. Rev. Lett. **87**, 146401 (2001).
45. J. Hubbard, Proc. Roy. Soc. London **A281** 238 (1963); ibid. **277**, 237;
M.C. Gutzwiller, Phys. Rev. Lett. **10**, 159 (1963);
J. Kanamori, Prog. Theor. Phys. **30**, 275 (1963).
46. U. Yu, K. Byczuk, and D. Vollhardt, in preparation.
47. K. Byczuk, M. Ulmke and D. Vollhardt, Phys. Rev. Lett. **90**, 196403 (2003).
48. K. Byczuk, W. Hofstetter and D. Vollhardt, Phys. Rev. **B69**, 045112 (2004).
49. K. Byczuk and M. Ulmke, Eur. Phys. J. **B45**, 449-454 (2005).
50. K. Byczuk, W. Hofstetter and D. Vollhardt, Phys. Rev. Lett. **94**, 056404 (2005).
51. J.K. Freericks and V. Zlatić, Rev. Mod. Phys. **75**, 1333 (2003).
52. K. Byczuk, Phys. Rev. **B71**, 205105 (2005).
53. K. Ziegler, arXiv:cond-mat/0611010.
54. Z. Gajek, J. Jedrzejewski and R. Lemanski, arXiv:cond-mat/9507122.
55. M.M. Maska and K. Czajka, Phys. Rev. **B74**, 035109 (2006).
56. V. Zlatic, J.K. Freericks, R. Lemanski and G. Czycholl, Phil. Mag. **B81**, 1443 (2001).
57. R. Lemanski, arXiv:cond-mat/0507474 and arXiv:cond-mat/0702415.
58. Wikipedia, the free encyclopedia:
http://en.wikipedia.org/wiki/Central_limit_theorem .
59. P.W. Anderson, Rev. Mod. Phys. **50**, 191 (1978).
60. P.S. Bullen, *Handbook of means and their inequalities*, (Kluwer Academic Publishers, 2003).
61. Wikipedia, the free encyclopedia:
http://en.wikipedia.org/wiki/Generalized_mean .
62. *Log-normal distribution–theory and applications*, Ed. E.L. Crow and K. Shimizu (Marcel Dekker, inc. 1988).
63. E.W. Montroll and M.F. Schlesinger, J. Stat. Phys. **32**, 209 (1983);
M. Romeo, V. Da Costa and F. Bardou, Eur. Phys. J. **B32**, 513 (2003).
64. K.A. Chao, J. Spalek and A. M. Oles, J. Phys. **C10**, L271 (1977).
65. K. Byczuk and D. Vollhardt, arXiv:0706.0839.
66. M.-T. Tran, Phys. Rev. B **73**, 205110 (2006); *ibid.* **76**, 245122 (2007).
67. R. Helmes, T.A. Costi, and A. Rosh, arXiv:0709.1669.
68. C. Töke, M. Snoek, I. Titvinidze, K. Byczuk, W. Hofstetter, in preparation.
69. M. Potthoff and W. Nolting, Phys. Rev. **B59**, 2549 (1999); Eur. Phys. J. **B8**, 555 (1999).
70. R. Bulla and M. Potthoff, Eur. Phys. J. **B13**, 257 (2000).
71. S. Okamoto and A.J. Millis, Phys. Rev. **B70**, 241104 (2004).
72. M. Eckstein, M. Kollar, K. Byczuk and D. Vollhardt, Phys. Rev. **B71**, 235119 (2005).
73. M. Kollar, M. Eckstein, K. Byczuk, N. Blümer, P. van Dongen, M.H. Radke de Cuba, W. Metzner, D. Tanaskovic, V. Dobrosavljevic, G. Kotliar and D. Vollhardt, Ann. Phys. (Leipzig) **14**, 642 (2005).

74. J.W. Negele and H. Orland, *Quantum many-particle systems*, (Perseus Book Publishing, L.L.C., 1998, 1988).
75. V. Turkowski and J.K. Freericks, arXiv:cond-mat/0612466.
76. R. Vlaming and D. Vollhardt, Phys. Rev. **B45**, 4637 (1992).
77. R.J. Elliott, J.A. Krumhansl and P.L. Leath, Rev. Mod. Phys. **46**, 465 (1974).
78. R. Bulla, Th. Costi and Th. Pruschke, arXiv:cond-mat/0701105.
79. W. Hofstetter, Advances in Solid State Physics **41**, 27 (2001).
80. J. Spalek, A. Datta and J.M. Honig, Phys. Rev. Lett. **59**, 728 (1987).
81. M. Ulmke, Eur. Phys. J. **B1**, 301 (1998).
82. J. Wahle, N. Blumer, J. Schlipf, K. Held and D. Vollhardt, Phys. Rev. **B58**, 12749 (1998).
83. D. Lloyd, J. Phys. **C2**, 1717 (1969);
D. Thouless, Phys. Reports **13**, 93 (1974);
F. Wegner, Z. Phys. **B44**, 9 (1981).
84. V. Dobrosavljević and G. Kotliar, Phys. Rev. Lett. **78**, 3943 (1997).
85. V. Dobrosavljević, A. A. Pastor and B. K. Nikolić, Europhys. Lett. **62**, 76 (2003).
86. G. Schubert, A. Weiße and H. Fehske, *High Performance Computing in Science and Engineering Garching 2004*, p. 237, Eds. A. Bode and F. Durst, (Springer Verlag, 2005).
87. V. Janiš and D. Vollhardt, Phys. Rev. **B46**, 15712 (1992);
M. Ulmke, V. Janiš and D. Vollhardt, Phys. Rev. **B51**, 10411 (1995).
88. F.X. Bronold, A. Alvermann and H. Fehske, Phil. Mag. **84**, 637 (2004).
89. A. Alvermann and H. Fehske, Eur. Phys. J. **B48**, 295 (2005).
90. M. Potthoff and M. Balzer, Phys. Rev. **B75**, 125112 (2007).
91. Yun Song, W.A. Atkinson and R. Wortis, arXiv:cond-mat/0609590.
92. A.M.C. Souza, D. de O. Maionchi and H.J. Herrmann, arXiv:cond-mat/0702355.
93. K. Byczuk, M. Kollar, K. Held, Y.-F. Yang, I.A. Nekrasov, Th. Pruschke and D. Vollhardt, Nature Physics **3**, 168 (2007).